

A meta-analysis assessing the cytotoxicity of nanoparticles on MCF7 breast cancer cells

ELCIN YENIDUNYA KONUK

Department of Medical Biology, Bakircay University School of Medicine, Menemen, İzmir 35665, Turkey

Received March 19, 2024; Accepted August 1, 2024

DOI: 10.3892/ol.2024.14684

Abstract. The present study summarizes the current available literature regarding the viability of MCF7 breast cancer cells treated with gold (Au), silver (Ag) or zinc oxide (ZnO) nanoparticles at varying doses for 48 h. The data for this study were obtained from diverse research articles published between 2013 and 2023 using Preferred Reporting Items for Systematic Reviews and Meta-Analyses (PRISMA) 2020 guidelines. The evaluation focused on 20 PRISMA-compliant articles concerning MCF7 cells, yielding 137 outcome measures for meta-analysis. A generalized linear mixed model meta-analysis approach was employed to glean insights into the effects of novel nanoparticles on MCF7 breast cancer cells. The analysis covered a wide range of concentrations: Ag nanoparticles from 1.25 to 1,000 $\mu\text{g/ml}$, Au nanoparticles from 50 to 150 $\mu\text{g/ml}$, and ZnO nanoparticles from 1 to 1,000 $\mu\text{g/ml}$. Both intra-nanoparticle and inter-nanoparticle comparisons were conducted to detect differences. The findings showed that when concentrations reached or exceeded 60 $\mu\text{g/ml}$, considerable variation of cell viability was observed: Treatment with Ag nanoparticles resulted in cell viability ranging from 9 to 45%, ZnO nanoparticles resulted in cell viability ranging from 20 to 40%, and Au nanoparticles resulted in cell viability ranging from 3 to 58%. These findings indicated the significance of thoroughly exploring nanoparticle dosage to acquire a comprehensive understanding of their influence on cell viability.

Introduction

In 2020, 2.3 million women worldwide were diagnosed with breast cancer and 685,000 breast cancer-related deaths occurred. From 2020 to January 2024, another 7.8 million

women have been diagnosed with breast cancer, making it the most prevalent cancer worldwide (1). Generally, cancer is characterized by abnormal tissue growth resulting from uncontrolled cell division, which leads to a progressive increase in the number of cells dividing autonomously (2). Notably, breast cancer is a complex disease that involves multiple stages of initiation, progression and metastasis; this necessitates a more comprehensive understanding and treatment approach for breast cancer.

Treatment with chemotherapy involves the induction of cell death to prevent the proliferation of cancer cells in the breast; however, normal cells are also affected. This limits chemotherapy treatment to a low-dose regimen that reduces effectiveness. Conversely, nanotechnology allows for the design of target-specific nanocarriers with a continuous drug release capacity, thus contributing to a reduction in the side effects of chemotherapeutic agents (3-5). Nanoparticles are a cornerstone of nanotechnology, which have garnered attention from researchers due to the development of new materials produced using noble metals, such as silver (Ag), platinum, gold (Au) and palladium, at the nanometer scale (6,7).

In vitro cytotoxicity testing procedures have also received attention due to their ability to reduce the reliance on laboratory animals (8), and have consequently promoted the use of cultured liposomes and cells (9). In this regard, the MCF7 and MCF10 cell lines have been reported to serve as valuable models, representing various critical steps in breast cancer progression (1). The MTT assay measures metabolic activity, such as cell viability, cytotoxicity and proliferation. This assay relies on the conversion of MTT by living cells into formazan crystals, allowing for the determination of mitochondrial activity. Given that total mitochondrial activity is generally correlated with the number of viable cells within the population, this assay is used in assessing the cytotoxic effects of drugs on cell lines or primary patient cells *in vitro* (2).

In the present study, an investigation was conducted to evaluate the effectiveness of active nanoparticles on the MCF7 breast cancer cell line over the last decade. This assessment encompassed an analysis of the administered dosages, the half-maximal inhibitory concentration (IC_{50}) values and the proportion of cell viability (determined using the MTT test), each with a specific focus on a 48-h incubation period. The aim of the present study was to provide a summary of the current available literature regarding the viability of cells in response to different nanoparticles, and to explore concentration levels

Correspondence to: Dr Elcin Yenidunya Konuk, Department of Medical Biology, Bakircay University School of Medicine, Kaynaklar Road, Gazi Mustafa Kemal, Menemen, İzmir 35665, Turkey
E-mail: elcin.yenidunya@bakircay.edu.tr; elcinyenidunya@gmail.com

Key words: meta-analysis, MCF7 cell line, nanoparticle, anticancer, cytotoxicity

for each nanoparticle over a 48-h period. It is anticipated that the present findings may contribute valuable insights into the development of novel nanoparticle-based treatments for breast cancer.

Materials and methods

Data collection. Data selection and meta-analysis followed the protocol outlined in the Preferred Reporting Items for Systematic Reviews and Meta-Analyses 2020 guidelines (10).

Criteria for database searching. A literature search was conducted within Science Direct (<https://www.sciencedirect.com/>), Scopus (<https://www.scopus.com/home.uri>) and PubMed (<https://pubmed.ncbi.nlm.nih.gov/>) to retrieve full-text research articles published between 2013 and 2023. Key words included 'MCF7', 'nanotechnology' and 'anti-cancer'. Journals were limited to the fields of chemistry, pharmacology, toxicology or pharmaceutical science.

Records excluded and included. Literature screening spanned from the beginning of 2022 through to September 2023. A total of 1,678 records were identified during the literature search (Fig. 1). Of these, 1,196 were from Science Direct, 41 were from Scopus and the remaining 441 were from PubMed. A total of 1,130 records were excluded as duplicates, leaving 548 to be screened. After implementing the eligibility criteria, an additional 290 cases were disqualified for various reasons. These included using nanoparticle combinations other than Ag, zinc oxide (ZnO) and Au, a lack of comparisons, and reporting varied parameter estimates unrelated to cell viability proportions. Furthermore, full-text articles were excluded if they deviated from the specific culture time (48 h), or if they presented unusual or specialized conditions (e.g. light irradiation in photodynamic therapy), or had ambiguous descriptions. This yielded 258 records that originated from 36 studies, each employing distinct nanoparticle dosages. Only results from studies with a 48-h culture time were included in the meta-analysis. Consequently, 15 studies from the original 36 were excluded from the dataset, removing 121 observations due to dosage discrepancies. This selection process led to 20 remaining studies and a cumulative total of 130 observations that were included in the meta-analysis. As shown in Table I, multiple doses were administered in each study. For example, Al-Khedhairi and Wahab (11) tested seven different doses ranging from 2 to 200 $\mu\text{g/ml}$ Ag. Similarly, Almalki and Khalifa (12) experimented with five different doses of Ag ranging from 10 to 50 $\mu\text{g/ml}$. When considering these instances collectively, a total of 130 different doses of Ag, ZnO and Au were tested across 20 studies, which formed the basis for the meta-analysis.

Data items. The outcome variable for the meta-analysis was the proportion of cell viability, derived from each nanoparticle group: Ag, ZnO and Au. Other variables included administered dosage and IC_{50} (measure of potency).

Establishing subgroups. The metal groups, along with dosages in the form of nanoparticles, formed the basis for the subgroup analyses. Dose applications for Ag ranged from 1.25 to

1,000 $\mu\text{g/ml}$; and the doses for Au and ZnO were 50-150 $\mu\text{g/ml}$ and 1-1,000 $\mu\text{g/ml}$, respectively. Dosages were categorized into homogeneous subgroups, considering the proportion of viable cells and IC_{50} values. In this context, Ag doses were distributed into the following five subgroups: <10, 10-15, 20-31, 40-50 and >60 $\mu\text{g/ml}$. Two groups were established for Au: 0.8-8 and ≥ 50 $\mu\text{g/ml}$. In the case of ZnO, four groups were formed: <10, 10-20, 30-40 and >50 $\mu\text{g/ml}$.

Statistical analysis. Primary outcomes, including data from various nanoparticles, applied dosages and IC_{50} values, were synthesized and presented using descriptive statistics in tables and forest plots. These analyses were performed with the 'meta' library (package) version 6.5 (July, 2023; <https://cran.r-project.org/web/packages/meta/index.html>), 'metafor' library (package) version 4.4-0 (September 27, 2023; <https://cran.r-project.org/web/packages/metafor/index.html>) in RStudio version 2023.06.0+421 (<https://posit.co/download/rstudio-desktop/>), as well as the RevMan 5.4.1 software (The Cochrane Collaboration; <https://training.cochrane.org/online-learning/core-software/revman>) and SAS (version 9.4; SAS Institute). In the present study, a robust statistical approach was employed to analyze the data, specifically focusing on the use of the generalized linear mixed model. More specifically, a random intercept logistic regression model with logit transformation was used for conducting a comprehensive meta-analysis of proportions. This statistical technique allowed the study to effectively address the challenges associated with synthesizing data across various studies, especially when dealing with binary outcomes or proportions. The random intercept logistic regression model accounts for both the within-study and between-study variability, making it well-suited for meta-analyses where the data comes from multiple sources with different characteristics and study designs. The logit transformation facilitates the modeling of proportions and the estimation of overall effects, enabling the study to derive meaningful insights and draw robust conclusions.

In the random-effects model, τ^2 was employed to assess the level of variation among the observed effects in distinct studies (between-study variance). This assessment is contingent upon the use of Cochran's homogeneity test, which is characterized by the Q statistic. The P-value associated with the test, which can be derived using either the Wald test or the likelihood ratio test (LRT), follows a χ^2 distribution with degrees of freedom equal to $k-1$, where k represents the number of studies included in the analysis (13). To gauge the consistency of results across individual studies, the I^2 test was employed. In this test, a score of <25% suggested a minimal level of between-study heterogeneity (14). Conversely, a higher I^2 score signified that the variation in effect estimates was not merely due to chance but indicated the potential influence of a moderator effect. Such a moderator effect can, to some extent, influence both the direction and the magnitude of the study's outcomes.

Notably, the random-effects model results were used for all reported results and evaluations, regardless of the I^2 value. This approach was in strict accordance with the Cochrane Handbook for Systematic Reviews of Interventions guidelines (13) (<https://training.cochrane.org/handbook>), ensuring consistency and rigor in the analysis and reporting of results.

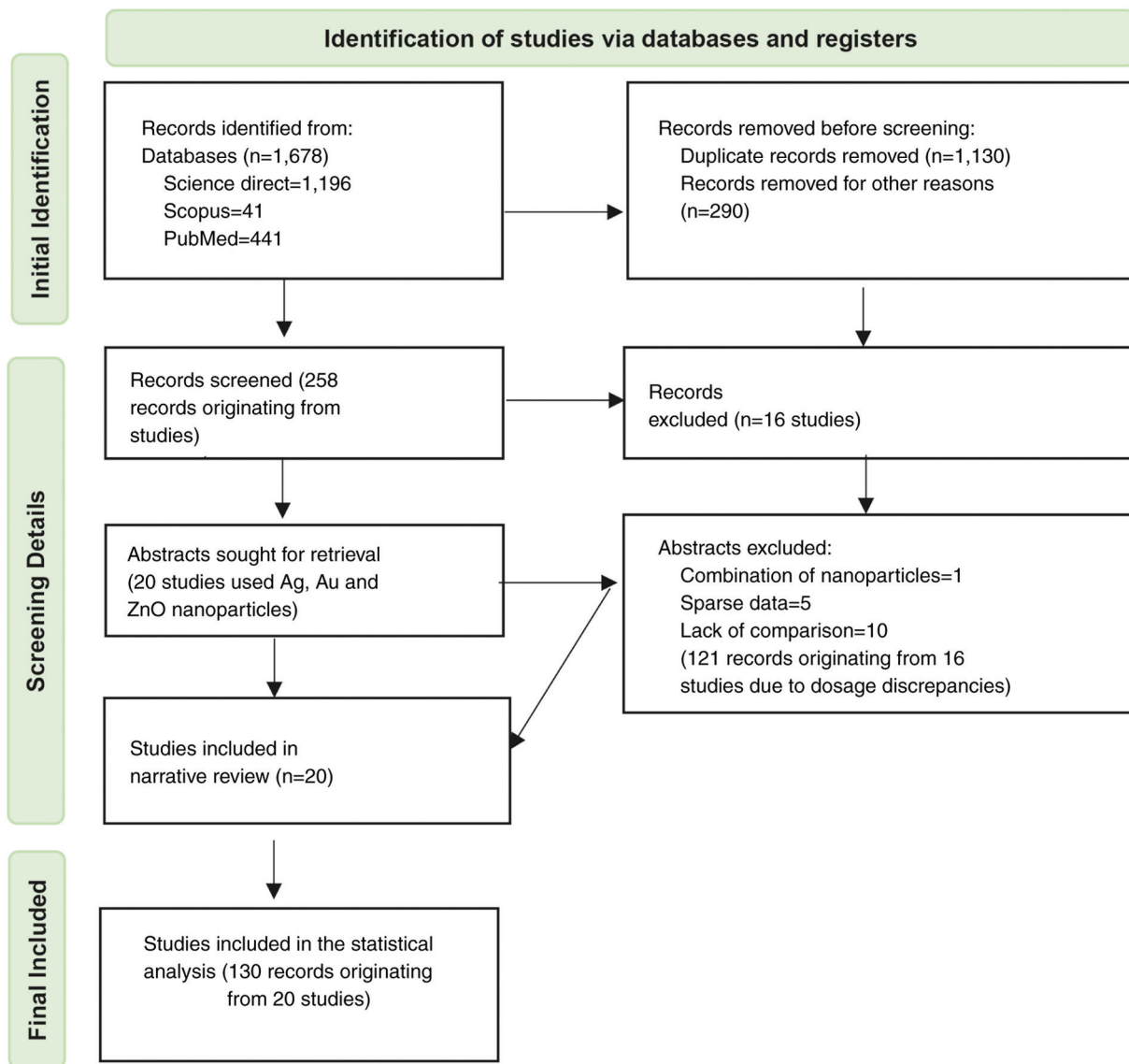


Figure 1. Flowchart for search strategy based on the 2020 Preferred Reporting Items for Systematic Reviews and Meta-Analyses guidelines. The flowchart illustrates the process of identifying and screening studies for inclusion in the review. The number of studies initially collected from Science Direct, Scopus and PubMed was 1,678. After removing duplicates and other irrelevant records, 258 records were screened from 36 studies and 16 studies were excluded at this stage because of reporting some combinations of nanoparticles. A total of 20 studies using Ag, Au and ZnO nanoparticles were sought for retrieval. Finally, 20 studies were included in the narrative review, with 130 records. Ag, silver; Au, gold; ZnO, zinc oxide.

Additionally, the forest plots were generated using the ‘meta’ library version 6.5 with the random-effects model applied by default.

To evaluate the source of heterogeneity, subgroups were created for nanoparticles, Ag, Au and ZnO; to better interpret the results, the random-effects meta-regression approach was employed. The Agresti-Coull interval approach that calculates confidence intervals for proportions was used for continuity of zero counts in any one cell. $P < 0.05$ was considered to indicate a statistically significant difference.

Results

Study characteristics: Detailed information regarding the 20 studies (11,12,15-31) and their characteristics is provided in Table I. The number of dosages investigated in these studies ranged from 1 to 16, resulting in a total of 130 data

points included in the meta-analyses. Among these studies, 16 reported outcomes related to Ag, three to Au and three to ZnO. The observed proportions of cell viability spanned the full spectrum from 0 to 100%, and IC_{50} values ranged from 1.5 to 200 $\mu\text{g/ml}$. Further insights and specifics about the included studies are included in Table I.

Separate meta-analyses with forest plots were conducted for the applied dose applications of Ag, Au and ZnO; however, due to the complexity of the findings the present analysis focused on the most notable results. As a consequence, three subgroup dosage comparisons were evaluated: i) Within the Ag group: $<10 \mu\text{g/ml}$ vs. $10\text{--}15 \mu\text{g/ml}$; ii) within the Ag group the lowest was compared to the highest dose: $<10 \mu\text{g/ml}$ vs. $\geq 60 \mu\text{g/ml}$; and iii) comparisons between Ag, Au and ZnO, all at $\geq 60 \mu\text{g/ml}$. To enhance the homogeneity and interpretability of the subgroup analysis comparing Ag, Au, and ZnO nanoparticles at $\geq 60 \mu\text{g/ml}$, the study by Sathishkumar *et al* (23)

Table I. Study characteristics.

First author, year	Nanoparticle used	Number of dosages used	IC ₅₀	Total cells counted	Proportion of viable cells, %	(Refs.)
Al-Khedhairy, 2022	Ag	7 (2-200 µg/ml)	5.18 µg/ml	1,000,000	9-100	(11)
Almalki, 2020	Ag	5 (10-50 µg/ml)	27-31 µg/ml	100,000	15-99	(12)
Balaji, 2022	ZnO	7 (5-60 µg/ml)	37 µg/ml	10,000	32-99	(15)
Charghadchi, 2021	Ag	8 (1.25-160 µg/ml)	13.4 µg/ml	100,000	10-77	(16)
Gomathi, 2020	Ag	9 (5-120 µg/ml)	20 µg/ml	10,000	15-98	(17)
Hashemi, 2021	Ag	6 (6.5-150 µg/ml)	21.28 µg/ml	10,000	10-90	(18)
Khandanlou, 2018	Au	5 (50-150 µg/ml)	116.65 µg/ml	10,000	3-72	(19)
Khedhairy, 2022	Ag	7 (2-200 µg/ml)	9.69 µg/ml	10,000	21-100	(11)
Krishnan, 2016	Ag	10 (2-200 µg/ml)	52 µg/ml	5,000	15-70	(20)
Mani, 2021	Ag	5 (25-200 µg/ml)	25-200 µg/ml	5,000,000	13.33-51.95	(21)
Nayaka, 2020	Ag	5 (12.5-200 µg/ml)	72.32 µg/ml	20,000	20-90	(22)
Sathishkumar, 2014	Ag	1 (5 µg/ml)	5 µg/ml	1,000,000	50	(23)
Shandiz, 2021	ZnO	4 (1-1,000 µg/ml)	7.23 µg/ml	10,000	0-65	(24)
Shawkey, 2013	Ag	16 (5-50 µg/ml)	22.4-30 µg/ml	100,000	41.3-100	(25)
Venugopal, 2016	Ag	10 (10-100 µg/ml)	52 µg/ml	5,000	15-80	(26)
Shewetha, 2020	ZnO	5 (20-100 µg/ml)	52.64 µg/ml	10,000	20-80	(27)
Solairaj, 2017	Ag	2 (31-1,000 µg/ml)	31 µg/ml	500,000	11.27-60	(28)
Ullah, 2020	Ag	7 (5-200 µg/ml)	25 µg/ml	20,000	10-62	(29)
Venugopal, 2017	Ag	14 (10-100 µg/ml)	60-70 µg/ml	5,000	15-80	(30)
Venugopal, 2021	Ag	5 (60-100 µg/ml)	60 µg/ml	5,000	15-45	(31)

Ag, silver; Au, gold; IC₅₀, half-maximal inhibitory concentration; ZnO, zinc oxide.

was excluded. This study employed a unique nanoparticle synthesis method and reported significantly different outcomes compared with the remaining studies.

Comparisons within the Ag group: <10 vs. 10-15 µg/ml. Fig. 2 presents the forest plot comparing Ag dosages <10 µg/ml to 10-15 µg/ml. The plot visualizes the ‘Events’ denoting the viable cell count and the total cell count, accompanied by their respective 95% confidence intervals (CIs). These proportions convey the impact of the administered Ag dosages on the proportion of viable cells. For example, Charghadchi *et al* (16) reported a proportion of 0.77 with a 95% CI of 0.767-0.773 for Ag dosages <10 µg/ml (Ag 1.25 µg/ml), while a proportion of 0.50 was observed with a 95% CI of 0.497-0.503 for dosages ranging from 10 to 15 µg/ml. Notably, similar results were observed in the study by Shawkey *et al* (25) for both Ag dosages. The summary statistics provide overall estimates of the effect. The ‘Random effects model’ estimated a proportion of cell viability of 0.967 (95% CI: 0.849-0.994) with a wider CI than fixed effect (0.769-0.770) and an I² value of 100%, indicating high variability between studies. This model assumes that the true effect may differ between studies.

In both Ag dosage groups and across all observations, substantial heterogeneity was evident. Notably, as an indicator of the dispersion between individual studies, the τ² values were elevated, reaching 37.30 for the <10 µg/ml Ag dosage group, 7.74 for the 10-15 µg/ml Ag dosage group, and 21.35 for the overall analysis. Heterogeneity was high, as indicated by an I² value of 100.0%. This finding underscores that all variations

observed in the results of the meta-analysis were attributed to genuine distinctions among the individual studies. Both the Wald test and the LRT unequivocally affirmed the presence of substantial heterogeneity, as denoted by a P<0.001. This robust statistical evidence firmly supports the notion that the effect sizes across studies are not uniform; thus, bolstering the rationale for employing the random-effects meta-analysis approach.

An extensive assessment was conducted to ascertain any notable distinctions between subgroups of Ag administered at doses <10 and 10-15 µg/ml. Both the fixed- and random-effects models were performed; in both instances, the significance level denoted a noteworthy contrast between the two subgroups, with a P<0.001 for the fixed-effects model (common effect) and a P=0.060 for the random-effects model (Fig. 2). This observation indicated the notable variation in the impact of the dosage and the associated trends between these two distinct groups.

Comparisons between the lowest and the highest doses of Ag: <10 vs. ≥60 µg/ml. In order to gain further insights from the results, a comparative analysis was conducted between the lower Ag dosages, which were <10 µg/ml, and dosages ≥60 µg/ml. The forest plot for this comparative analysis is depicted in Fig. 3. The results demonstrated a notable variation in the proportions of viable cells in response to different Ag dosages. Specifically, for Ag concentrations <10 µg/ml, the observed proportions ranged from 0.50 to 1.00. By contrast, for Ag dosages ≥60 µg/ml, the proportions of viable cells fell

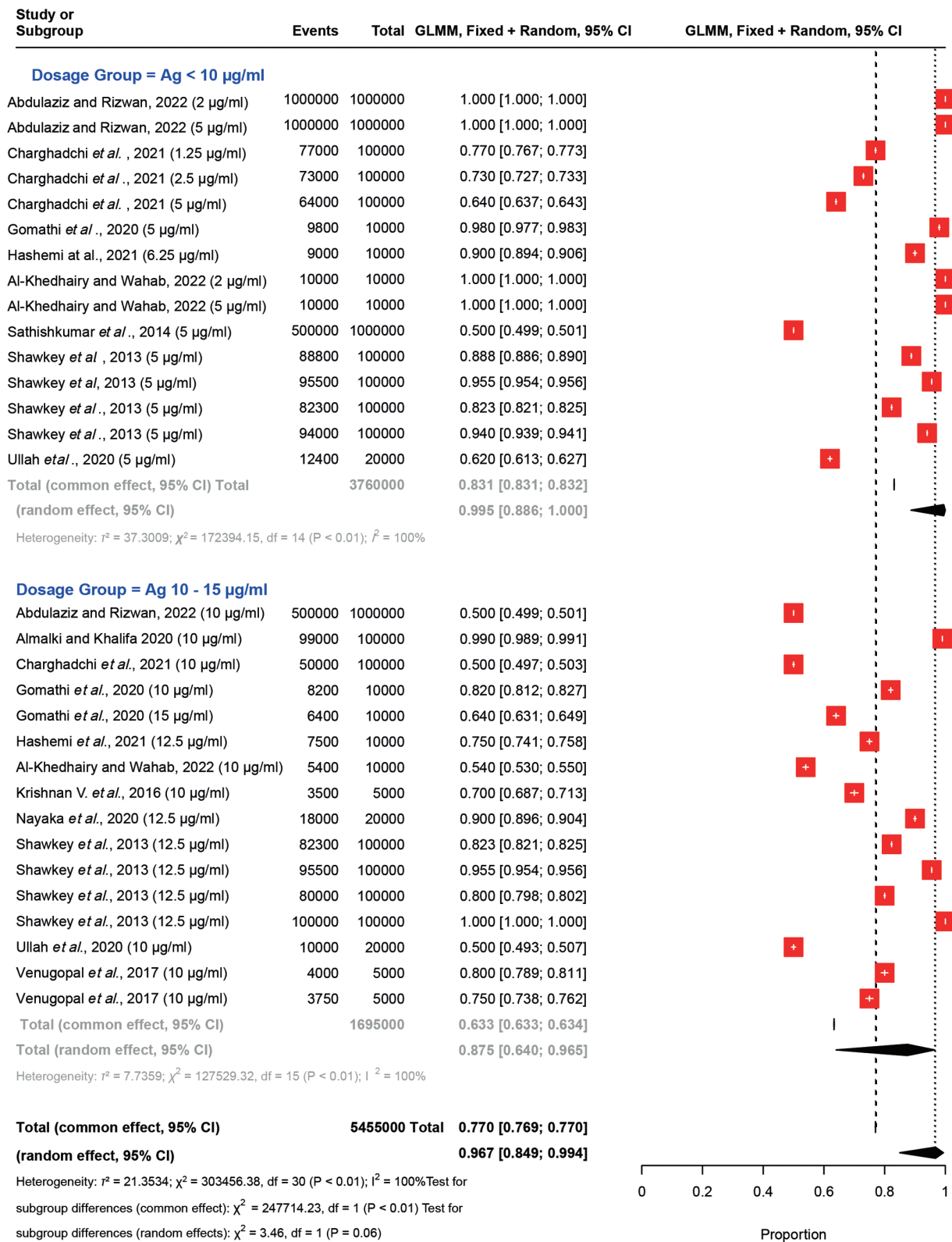


Figure 2. Forest plots for comparing Ag nanoparticles at dosages of <10 and 10-15 µg/ml. Each study is represented by a red square indicating the effect estimate and its 95% CI. The size of the square reflects the weight of the study in the meta-analysis. For each dosage group, the plot shows the individual study estimates, the total common effect (fixed-effects model), and the total random effect (random-effects model) with their 95% CIs. Heterogeneity statistics (τ^2 , χ^2 , I^2) are provided for both dosage groups and overall. The overall effect estimate is represented by a diamond at the bottom of the plot, with the width of the diamond representing the 95% CI. Ag, silver; CI, confidence interval; GLMM, generalized linear mixed model.

within the range of 0.09 to 0.45. These results demonstrated the impact of Ag dosages on the proportions of viable cells. For example, Al-Khedhairi and Wahab (11) revealed that in

response to Ag concentrations <10 µg/ml, the proportion was consistently 1.00 (100%) with a narrow CI. In response to Ag dosages ≥ 60 µg/ml, the proportion remained at 0.09 (9%)

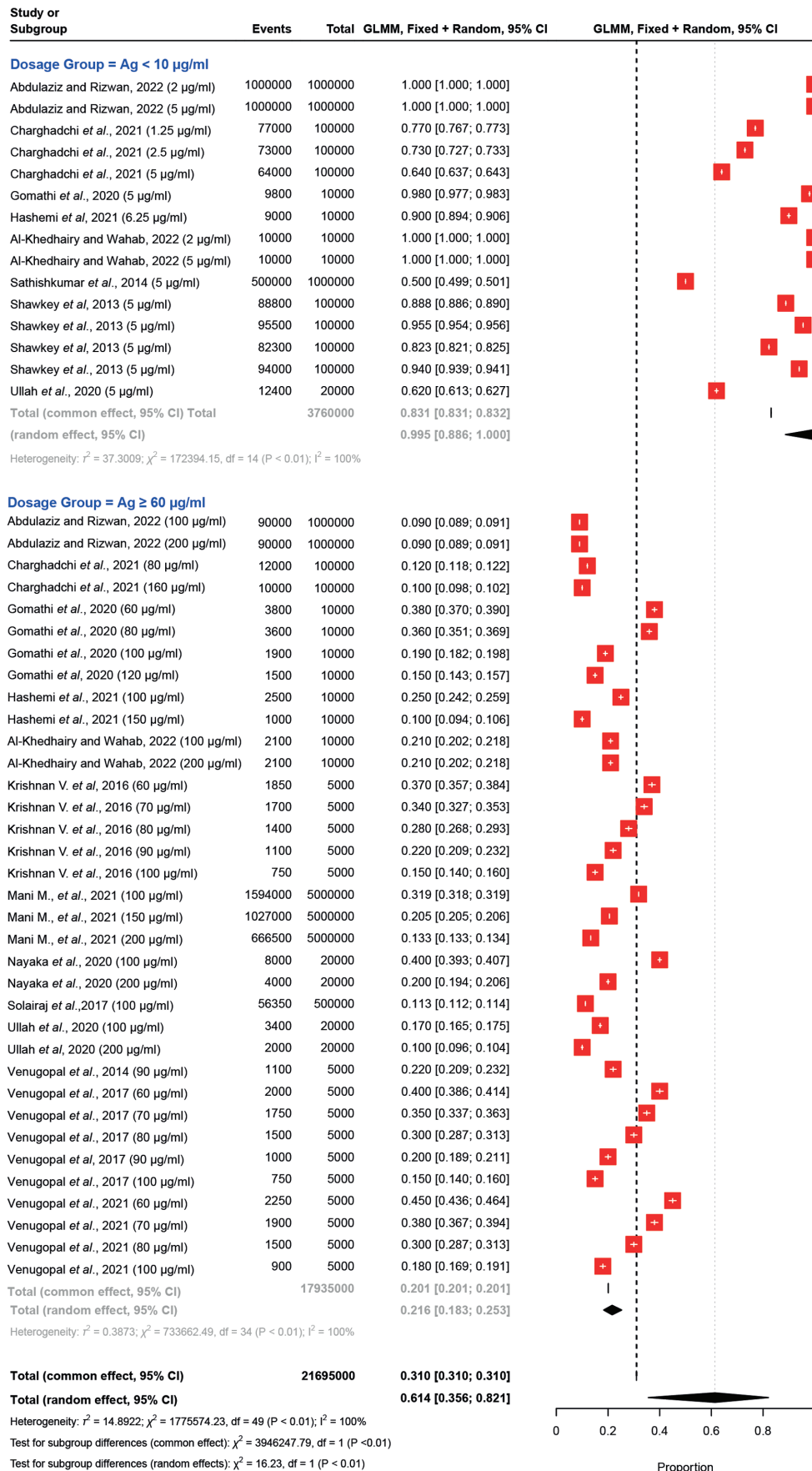


Figure 3. Forest plots for comparing Ag nanoparticles at dosages of <10 and ≥60 µg/ml. Each study is represented by a red square indicating the effect estimate and its 95% CI, with the size of the square reflecting the study weight. The plot includes individual study estimates, the total common effect (fixed-effects model), the total random effect (random-effects model), and heterogeneity statistics (τ^2 , χ^2 , I^2) for each group and overall. The overall effect estimate for each group is depicted by a diamond at the bottom of the plot, with the width of the diamond representing the 95% CI. Ag, silver; CI, confidence interval; GLMM, generalized linear mixed model.

with narrow CIs. These findings are similar to those across other studies and dosage groups (26). The analysis conducted on the forest plot provides a comprehensive assessment of heterogeneity within the dataset. Several statistical measures were utilized, including τ^2 , I^2 and Higgins' I^2 adjusted for the number of studies, to gauge the extent of heterogeneity. The results indicated significant heterogeneity among the studies, as affirmed by both the Wald test and the LRT, both yielding, $\chi^2 = 16.23$, $P < 0.01$ (Fig. 3).

In the random-effects model, distinct patterns emerged. Ag concentrations $< 10 \mu\text{g/ml}$ exhibited a viable-cell proportion of 0.9946 (99%), coupled with a high estimated τ^2 (37.3009) value, indicating substantial heterogeneity within this subgroup. The high τ^2 suggested that there was significant variability in effect sizes among the included studies, beyond what would be expected by chance alone.

By contrast, Ag dosages $\geq 60 \mu\text{g/ml}$ demonstrated a viable-cell proportion of 0.2161 (22%) with a relatively lower estimated τ^2 value (0.3873), suggesting less heterogeneity within this subgroup. The lower τ^2 indicates that the effect sizes across the included studies are more consistent and similar, with less variability than would be expected by chance. This consistency may imply that the studies in this subgroup share more common characteristics or that the outcome is more stable across different settings.

Comparisons between Ag, Au and ZnO, all at $\geq 60 \mu\text{g/ml}$. A comparison by group (Ag, Au and ZnO) at concentrations $\geq 60 \mu\text{g/ml}$ was conducted, as a sufficient number of studies was available for each nanoparticle type. The results for these comparisons are shown in Fig. 4. The proportion of cell viability for both Ag and ZnO ranged from 0.09 to 0.40; whereas Au exhibited proportions between 0.03 and 0.58. These results indicated the significant variation in the effects of different nanoparticle dosages on cell viability when $\geq 60 \mu\text{g/ml}$ was applied. These findings revealed the diverse impacts of various nanoparticle dosages on the proportion of viable cells, emphasizing the importance of considering dosage levels in nanoparticle studies.

Discussion

The present meta-analysis provides additional insights into the impact of Ag, Au and ZnO nanoparticles on the viability of MCF7 cells, exploring diverse concentration levels for each nanoparticle over a 48-h period. Within the scope of MCF7 cells, previous studies (9-12) have illustrated the effects of nanoparticles formulated with distinct active agents, examining either the nanoparticle itself or its potential anticancer properties. Analyzing results from studies encompassing the most prevalent metals in nanoparticle synthesis, Ag, Au and ZnO, revealed similar results in the proportions of viable MCF7 cells when exposed to Ag, Au and ZnO nanoparticles at concentrations $\geq 60 \mu\text{g/ml}$. These findings are consistent for data derived from live cell rates obtained through the MTT test after a 48-h incubation period. The present meta-analysis provided additional evidence regarding the effect of Ag, Au and ZnO nanoparticles on the proportion of viable MCF7 cells using different concentrations of each nanoparticle for 48 h.

In the studies conducted by Sathishkumar *et al* (23), Ullah *et al* (29) and Charghadchi *et al* (16), the proportion

of viable cells was determined to be 50, 62 and 64% for $< 10 \mu\text{g/ml}$ Ag, respectively. Nevertheless, the outcomes of the meta-analysis revealed that, following a 48-h incubation period with $< 10 \mu\text{g/ml}$ Ag nanoparticles, the overall average proportion of cell viability was 0.995 (95% CI, 0.888-1.000). The heterogeneity within the studies of this group was quantified by τ^2 , yielding a value of 37.3009. Significance is attributed to this heterogeneity, as determined by the χ^2 test ($P < 0.05$). The foremost contributors to the observed heterogeneity were considered to be the three aforementioned studies. When comparing data within the Ag group (i.e., < 10 vs. $10-15 \mu\text{g/ml}$), a $< 10 \mu\text{g/ml}$ Ag dosage was utilized in multiple studies (11,16,18,19,23,25,29).

These studies not only synthesized Ag nanoparticles but also incorporated diverse extracts into the experimental design during their creation. Consequently, the observed heterogeneity suggests that the variability in results regarding Ag nanoparticle concentrations $< 10 \mu\text{g/ml}$ could be attributed to the different active substances used alongside Ag. This indicates that the combination of Ag with other substances may lead to differing effects, contributing to the diversity of outcomes observed.

The present meta-analysis aimed to elucidate the cytotoxic effects of Ag, Au and ZnO nanoparticles on MCF7 breast cancer cells. The findings indicated that all three nanoparticles exhibited marked cytotoxicity at higher concentrations ($\geq 60 \mu\text{g/ml}$). Specifically, Ag nanoparticles reduced cell viability to a range between 9 and 45%; ZnO nanoparticles reduced viability to between 20 and 40%; and Au nanoparticles exhibited a broader range of viability, from 3 to 58%. This variability underscores the distinct cytotoxic potentials of each nanoparticle type (32).

In the framework of the random-effects meta-analysis model, the mean proportion of viable cells 48 h post-application of Ag doses ranging from 10 to $15 \mu\text{g/ml}$ was determined to be 0.875 (95% CI, 0.640-0.965). The heterogeneity value within this specific group was $\tau^2 = 7.7359$, reaching statistical significance through the χ^2 test ($P < 0.01$). Notably, studies conducted within this subgroup have introduced diverse active substances into Ag nanoparticles (12,16,18,20). The observed heterogeneity in this category may be due to the varied use of active substances, such as *Allium cepa* leaf extract, chitin and *Syzygium aromaticum* (clove). To allow the homogeneity and interpretability of the subgroup analysis, the study by Sathishkumar *et al* (23) was excluded from the comparison of Ag, Au and ZnO nanoparticles at $\geq 60 \mu\text{g/ml}$. This omission represents an intriguing observation as it allows for a more focused examination of the data within this specific concentration range.

The results of the random-effects meta-analysis indicated that as the applied dose concentration of Ag nanoparticles increased, a rapid decline in the average cell viability became evident. For example, additional analyses using different assays, which were not depicted here, revealed that the mean live cell ratio in response to 20 and $31 \mu\text{g/ml}$ Ag was 0.66 (95% CI, 0.52-0.77), whereas the mean live cell ratio was observed to be 0.60 (95% CI, 0.30-0.84) for doses between 35 and $50 \mu\text{g/ml}$ Ag, and 0.22 (95% CI, 0.18-0.25) for doses at $50 \mu\text{g/ml}$ Ag (data not shown). Factors contributing to the cytotoxicity induced by Ag nanoparticles may include the initiation of apoptosis through the

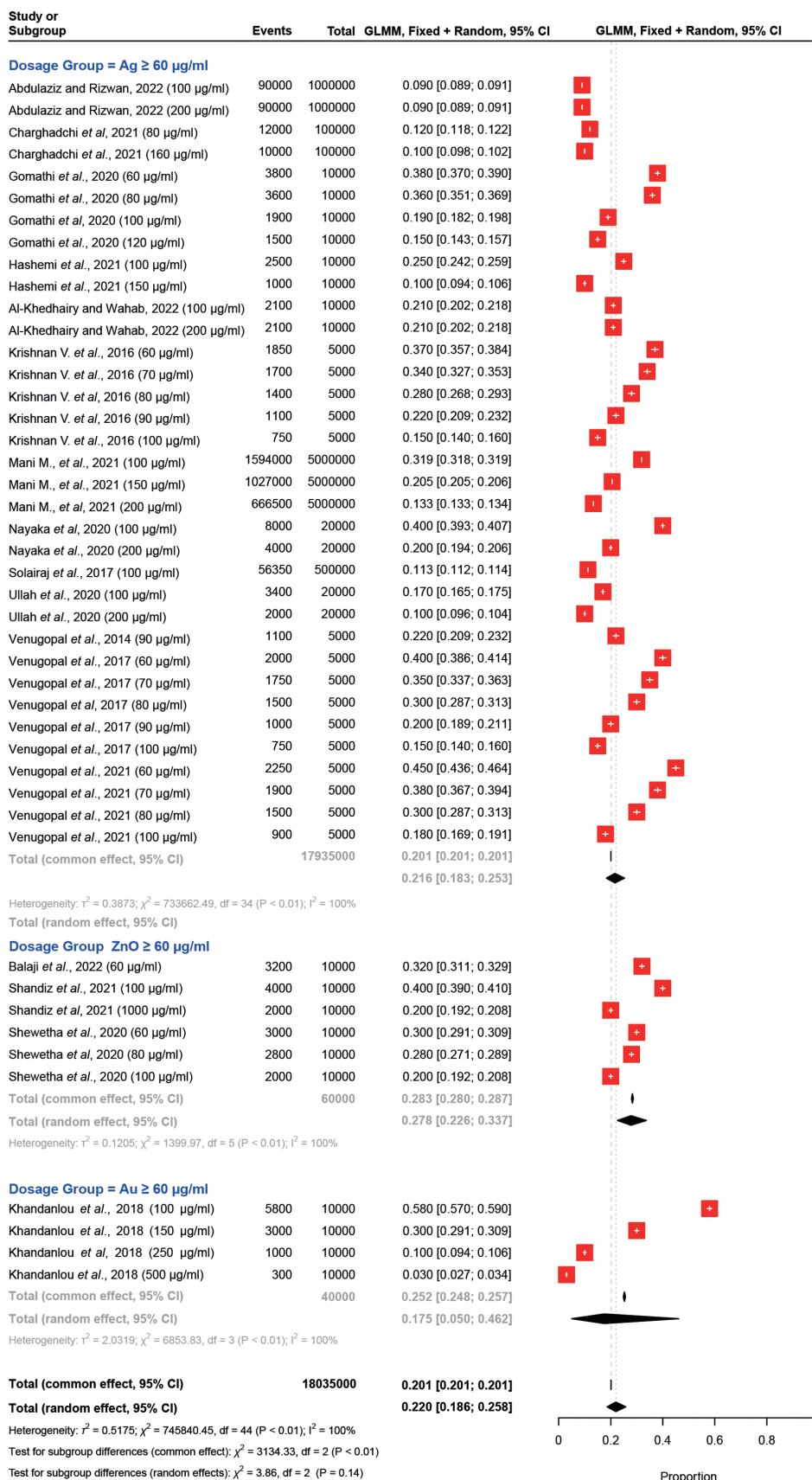


Figure 4. Forest plots for ≥60 µg/ml dosages of Ag, ZnO, and Au nanoparticles. The effects of Ag, ZnO and Au nanoparticles at ≥60 µg/ml were compared on breast cancer cell viability *in vitro*. Each study or subgroup is represented by nanoparticle type, observed events (cell viability) out of the total cells studied, and the proportion of viable cells with 95% CIs derived from a random-effects model. The red square indicates the effect estimate and its 95% CI, with the size of the square reflecting the study weight. The plot includes individual study estimates, the total common effect (fixed-effects model), the total random effect (random-effects model) and heterogeneity statistics (τ^2 , χ^2 , I^2) for each group and overall. The overall effect estimate for each group is depicted by a diamond at the bottom of the plot, with the width of the diamond representing the 95% CI. Ag, silver; Au, gold; CI, confidence interval; GLMM, generalized linear mixed model; ZnO, zinc oxide.

mitochondrial pathway in various cell lines, the production of reactive oxygen species through lipid peroxidation in biological membranes, and the induction of damage in structural proteins and DNA (7,32). In a study conducted by Liu *et al* (33) on MCF7 cells, it was determined that the size and surface area of the used Ag nanoparticles influenced cytotoxicity. Furthermore, Ag nanoparticles induce apoptosis and necrosis at lower concentrations (<6 $\mu\text{g/ml}$), but only lead to necrosis at higher concentrations (>65 $\mu\text{g/ml}$) (34). A crucial consideration for the clinical application of these findings is whether the effective *in vitro* concentrations can be replicated. The concentrations exhibiting marked cytotoxic effects ($\geq 60 \mu\text{g/ml}$) must be achievable in both plasma and tumor tissues to ensure therapeutic efficacy. For Ag, Au and ZnO nanoparticles to be clinically viable, it is essential to evaluate their pharmacokinetics and biodistribution *in vivo*. Studies have shown that nanoparticles can accumulate in tumor tissues through the enhanced permeability and retention effect, but achieving therapeutic concentrations while minimizing systemic toxicity remains a challenge (35). As homogeneous groups, defined as groups with similar characteristics or conditions, could not be established within the dose applications of <60 $\mu\text{g/ml}$ for Au and ZnO due to the limited number of available studies, the present study focused on evaluating cell viability rates 48 h after administering doses of Ag, Au and ZnO nanoparticles at $\geq 60 \mu\text{g/ml}$. This was done in conjunction with assessing three distinct nanoparticles. The mean proportion of cell viability in response to ZnO nanoparticles at doses $\geq 60 \mu\text{g/ml}$ were recorded at 0.278 (95% CI, 0.226-0.337). By contrast, the mean proportions of cell viability in response to Ag and Au at doses $\geq 60 \mu\text{g/ml}$ were 0.22 (95% CI, 0.18-0.25) and 0.18 (95% CI, 0.05-0.46), respectively. When considering the three nanoparticles assessed in the present study, it was evident that Au exhibited higher heterogeneity and variability in studies involving doses $\geq 60 \mu\text{g/ml}$ compared with the other two nanoparticles. The increased use of extracts in conjunction with Ag in the evaluated studies has led to greater heterogeneity and variability compared with the other two particles. In the meta-analyses conducted, the studies employed a diverse range of active substances in combination with Ag. For example, among the 11 studies that used Ag, only two used Ag alone, accounting for 18.2%. Similarly, out of the three studies that used ZnO nanoparticles, only one used ZnO alone (33.33%). On the other hand, studies involving Au conducted experiments without using extracts. Notably, the CI obtained for the live cell ratios of Ag nanoparticles at doses $\geq 60 \mu\text{g/ml}$ was less extensive compared with that obtained for the other two nanoparticles. While 34 results from 11 studies were reported for Ag nanoparticles at doses $\geq 60 \mu\text{g/ml}$, ZnO nanoparticles yielded six results from three studies, and Au nanoparticles reported four results from a single study across four different doses. The differing results observed across studies examining Au nanoparticles may arise from several factors, including differences in nanoparticle size, coating materials, experimental conditions and the biological systems used in the studies. Moreover, previous research has indicated that Ag nanoparticles can reach therapeutic levels in plasma and tumor tissues but require careful dosing to avoid systemic toxicity. Au nanoparticles, noted for their biocompatibility and potential for targeted delivery, show promise in achieving high tumor concentrations, although precise dosage optimization is

necessary due to variable cytotoxic effects. ZnO nanoparticles, which were associated with moderate cytotoxicity and a higher proportion of viable cells in response to $\geq 60 \mu\text{g/ml}$, may have a wider therapeutic window but may be less effective compared with Ag and Au nanoparticles (36,37).

The heterogeneity observed in the present study has been suggested to be influenced by several factors, including the application of the MTT colorimetric method to measure the proportion of viable cells. The MTT method was applied to groups categorized based on administered doses, synthesis methods affecting particle size, shape and surface properties, as well as study design and conditions. Variations in nanoparticle synthesis methods for Ag, Au and ZnO nanoparticles may also have contributed to this heterogeneity. This study offers valuable insights for researchers planning future investigations by highlighting key factors and considerations that may influence study outcomes. It identifies potential sources of variability that involve the use of nanoparticles in combination with anticancer agents. The findings suggested that Ag and Au nanoparticles exhibit superior cytotoxic effects compared with ZnO nanoparticles at similar concentrations. This insight may guide future research on nanoparticle-based therapies for breast cancer. Further *in vivo* studies are necessary to determine the optimal dosing regimens, and to evaluate the long-term safety and efficacy of these nanoparticles. Additionally, the development of targeted delivery systems could enhance the accumulation of nanoparticles in tumor tissues, thereby increasing their therapeutic potential while minimizing systemic side effects. Future research should also explore combination therapies, where nanoparticles are used alongside conventional treatments to enhance overall efficacy. In summary, the present study highlighted the significant cytotoxic potential of Ag, Au and ZnO nanoparticles on MCF7 breast cancer cells. Ag and Au nanoparticles, in particular, demonstrated superior cytotoxic effects at higher concentrations. Achieving these effective concentrations *in vivo* remains a critical challenge that must be addressed to realize the clinical potential of these therapies. Future research should focus on optimizing nanoparticle formulations, dosing strategies and delivery mechanisms to translate these promising *in vitro* findings into viable clinical applications.

One of the limitations of the present study is the exclusive use of the MTT assay to assess cell viability, without including other viability and apoptosis assays, such as CellTiter-Blue, Caspase-Glo 3/7 and TUNEL. The inclusion of multiple assays could have provided a more comprehensive understanding of cell viability and apoptotic mechanisms. Each assay has its unique sensitivity and specificity, and a combination of these could have validated and reinforced the findings. However, the decision to include only the MTT assay was intentional. During the literature review, it was observed that the MTT assay was the most consistently reported across the selected studies. Additionally, the MTT assay, which was used in all of the studies, is a well-established method for assessing cell metabolic activity and viability, providing reliable and reproducible results (2,11,34). This consistency in reporting enabled for more direct comparisons between the findings. Additionally, the MTT assay is a well-established method for assessing cell metabolic activity and viability, providing reliable and reproducible results. By focusing on a single, widely-used assay, it was aimed to ensure that the results were comparable to the majority of existing studies, thus

maintaining the integrity and relevance of the present findings within the broader context of current research.

Another limitation of the present study was the exclusive use of MCF7 cells, a specific type of breast cancer cell line, without including other breast cancer cell lines. The inclusion of various breast cancer cell lines may have offered a broader perspective on the efficacy and mechanism of the treatment across different cellular contexts. The choice to use only MCF7 cells was based on their extensive use in breast cancer research, which allows for better comparisons with previously published data. MCF7 cells are well-characterized, and have been widely used as a model system to study breast cancer biology and treatment responses. However, future studies should include a range of breast cancer cell lines to enhance the generalizability of the findings.

Furthermore, the present study did not include normal non-transformed cell lines, such as MCF10A, to determine whether the nanoparticles selectively targeted cancer cells or also affected normal cells. Including normal cell lines could provide insights into the selectivity and potential toxicity of the treatment, which is crucial for assessing its safety profile. The decision to exclude normal cell lines was made to focus on the primary objective of evaluating the efficacy of the treatments against breast cancer cells. Nevertheless, assessing the impact on normal cells is essential for future studies to ensure the therapeutic selectivity and minimize potential side effects.

In conclusion, the present study offers important insights into the effects of treatment on breast cancer cells. However, the limitations related to the choice of assays, the diversity of cell lines and the absence of normal cell lines underscore the need for further research. Future studies that incorporate a variety of assays, different cancer cell lines and normal cells will strengthen the reliability and relevance of the results.

Acknowledgements

The author would like to thank Ms. Rosey Zackula (School of Medicine, University of Kansas, Wichita, Kansas, USA) for their guidance regarding PRISMA, support in structuring the article and contributions to grammar. Furthermore, the author would like to acknowledge Dr Hayrettin Okut (School of Medicine, University of Kansas, Wichita, Kansas, USA) for their participation in conducting the meta-analysis using RStudio.

Funding

No funding was received.

Availability of data and materials

The data generated in the present study may be requested from the corresponding author.

Authors' contributions

EYK conceived and designed the study, carried out the data collection, performed the data analysis and interpreted the results of the statistical analysis. The author confirmed the authenticity of all the raw data. The author read and approved the final version of the manuscript.

Ethics approval and consent to participate

Not applicable.

Patient consent for publication

Not applicable.

Competing interests

The author declares that they have no competing interests.

References

1. World Health Organization (WHO): Breast Cancer. WHO, Geneva, 2024. <https://www.who.int/news-room/fact-sheets/detail/breast-cancer>. Accessed July 3, 2024.
2. van Meerloo J, Kaspers GJL and Cloos J: Cell sensitivity assays: The MTT assay. *Methods Mol Biol* 731: 237-245, 2011.
3. Chen X, Fan N, Tan H, Ren B, Yuan G, Jia Y, Li J, Xiong D, Xing X, Niu X and Hu X: Magnetic and self-healing chitosan-alginate hydrogel encapsulated gelatin microspheres via covalent cross-linking for drug delivery. *Mater Sci Eng C Mater Biol Appl* 101: 619-629, 2019.
4. Dalwadi C and Patel G: Thermosensitive nanohydrogel of 5-fluorouracil for head and neck cancer: Preparation, characterization and cytotoxicity assay. *Int J Nanomedicine* 13: 31-33, 2018.
5. Krutyakov YA, Kudrinskiy AA, Olenin AY and Lisichkin GV: Synthesis and properties of silver nanoparticles: Advances and prospects. *Russ Chem Rev* 77: 233, 2008.
6. Chaloupka K, Malam Y and Seifalian AM: Nanosilver as a new generation of nanoparticle in biomedical applications. *Trends Biotechnol* 28: 580-588, 2010.
7. Lee DG, Go EB, Lee M, Pak PJ, Kim J and Chung N: Gold nanoparticles conjugated with resveratrol induce cell cycle arrest in MCF7 cell lines. *Appl Biol Chem* 62: 33, 2019.
8. Abraham SA, McKenzie C, Masin D, Ng R, Harasym TO, Mayer LD and Bally MB: In vitro and in vivo characterization of doxorubicin and vincristine coencapsulated within liposomes through use of transition metal ion complexation and pH gradient loading. *Clin Cancer Res* 10: 728-738, 2004.
9. Byrd JC, Lucas DM, Mone AP, Kitner JB, Drabick JJ and Grever MR: KRN5500: A novel therapeutic agent with in vitro activity against human B-cell chronic lymphocytic leukemia cells mediates cytotoxicity via the intrinsic pathway of apoptosis. *Blood* 101: 4547-4550, 2003.
10. Page MJ, McKenzie JE, Bossuyt PM, Boutron I, Hoffmann TC, Mulrow CD, Shamseer L, Tetzlaff JM, Akl EA, Brennan SE, *et al*: The PRISMA 2020 statement: An updated guideline for reporting systematic reviews. *BMJ* 372: n71, 2021.
11. Al-Khedhairi AA and Wahab R: Silver nanoparticles: An instantaneous solution for anticancer activity against human liver (HepG2) and breast (MCF7) cancer cells. *Metals* 12: 148, 2022.
12. Almalki MA and Khalifa AYZ: Silver nanoparticles synthesis from *Bacillus* sp KFU36 and its anticancer effect in breast cancer MCF-7 cells via induction of apoptotic mechanism. *J Photochem Photobiol B* 204: 111786, 2020.
13. Welch VA, Petkovic J, Jull J, Hartling L, Klassen T, Kristjansson E, Pardo Pardo J, Petticrew M, Stott DJ, Thomson D, *et al*: Chapter 16: Equity and specific populations. In: *Cochrane Handbook for Systematic Reviews of Interventions*. 2nd edition. Cochrane, pp435-448, 2019.
14. West SL, Gartlehner G, Mansfield AJ, Poole C, Tant C, Lenfestey N, Lux LJ, Amoozegar J, Morton SC, Carey TC, *et al*: Comparative effectiveness review methods: Clinical heterogeneity [Internet]. Agency for Healthcare Research and Quality (US), Rockville, MD, 2010. <https://www.ncbi.nlm.nih.gov/books/NBK53317/table/ch3.t2/>.
15. Balaji MP, Govindasamy R, Alharbi NS, Kadaikunnan S, Thiruvengadam M, Baskar V and Rajeswari VD: Biosynthesis of ZnONP using *Chamaecostus cuspidatus* and their evolution of anticancer property in MCF-7 and A549 cell lines. *Nanomaterials (Basel)* 12: 3384, 2022.

16. Charghadchi M, Gharari Z, Sadighian S, Yazdinezhad A and Sharafi A: Green synthesized silver nanostructure using rhus coriaria fruit extract inhibits the growth of malignant MCF7 Cell Line. *Braz Arch Biol Technol* 64: e21210069, 2021.
17. Gomathi AC, Rajarathinamb SRX, Sadiq AM and Rajeshkumar S: Anticancer activity of silver nanoparticles synthesized using aqueous fruit shell extract of Tamarindus indica on MCF7 human breast cancer cell line. *J Drug Deliv Sci Technol* 55: 101376, 2020.
18. Hashemi Z, Mohammadyan M, Naderi S, Fakhari M, Biparva P, Akhtari J and Ebrahimzadeh MA: Green synthesis of silver nanoparticles using Ferula persica extract (Fp-NPs): Characterization, antibacterial, antileishmanial, and in vitro anticancer activities. *Mater Today Commun* 27: 102264, 2021.
19. Khandanlou R, Murthy V, Saranath D and Damani H: Synthesis and characterization of gold-conjugated Backhousia citriodora nanoparticles and their anticancer activity against MCF7 breast and HepG2 liver cancer cell lines. *J Mater Sci* 453: 3106-3118, 2018.
20. Krishnan V, Bupesh G, Manikandan E, Thanigai Arul K, Magesh S, Kalyanaraman R and Maaza M: Green synthesis of silver nanoparticles using piper nigrum concoction and its anticancer activity against MCF7 and Hep-2 cell lines. *J Antimicrob* 2: 3, 2016.
21. Mani M, Okla MK, Selvaraj S, Ram Kumar A, Kumaresan S, Muthukumaran A, Kaviyarasu K, El-Tayeb MA, Elbadawi YB, Almaary KS, et al: A novel biogenic *Allium cepa* leaf mediated silver nanoparticles for antimicrobial, antioxidant, and anticancer effects on MCF-7 cell line. *Environ Res* 198: 111199, 2021.
22. Nayaka S, Bhat SMP, Chakraborty B, Pallavi SS, Airodagi D, Muthuraj R, Halaswamy HM, Dhanyakumara SB, Shashiraj KN and Kupaneshi C: Seed extract-mediated synthesis of silver nanoparticles from Putranjiva roxburghii Wall., phytochemical characterization, antibacterial activity and anticancer activity against MCF7 cell line. *Indian J Pharm Sci* 82: 260-269, 2020.
23. Sathishkumar G, Gobinath C, Wilson A and Sivaramakrishnan S: Dendrophthoe falcata (L.f) Ettingsh (Neem mistletoe): A potent bioresource to fabricate silver nanoparticles for anticancer effect against human breast cancer cells (MCF7). *Spectrochim Acta A Mol Biomol Spectrosc* 128: 285-290, 2014.
24. Shandiz SAS, Sharifian F, Behboodi S, Ghodrathpour F and Baghbani-Arani F: Evaluation of metastasis suppressor genes expression and in vitro anti-cancer effects of zinc oxide nanoparticles in human breast cancer cell lines MCF7 and T47D. *Avicenna J Med Biotechnol* 13: 9-14, 2021.
25. Shawkey AM, Rabeh MA, Abdulall AK and Abdellatif AO: Green nanotechnology: anticancer activity of silver nanoparticles using citrullus colocynthis aqueous extracts. *Adv Life Sci Technol* 13: 60-70, 2013.
26. Venugopal K, Shanthi MP, Rajagopal K, Bhaskar M, Uvarajan S and Manikandan E: Bioactivity of cancer cells (MCF-7 and Hep-2) using plant extract enhanced surface plasmon resonance (SPR) nanoparticles (Ag NPs). <https://www.researchgate.net/publication/312164782>.
27. Shewetha UR, Latha MS, Rajith Kumar CR, Kiran MS and Betageri VS: Facile synthesis of zinc oxide nanoparticles using novel areca catechu leaves extract and their in vitro antidiabetic and anticancer studies. *J Inorg Organomet Polym Mater* 30: 4876-4883, 2020.
28. Solairaj D, Rameshthangam P and Arunachalam G: Anticancer activity of silver and copper embedded chitin nanocomposites against human breast cancer (MCF-7) cells. *Int J Biol Macromol* 105: 608-619, 2017.
29. Ullah I, Khalil AT, Ali M, Iqbal J, Ali W, Alarifi S and Shinwari ZH: Green-synthesized silver nanoparticles induced apoptotic cell death in MCF-7 breast cancer cells by generating reactive oxygen species and activating caspase 3 and 9 enzyme activities. *Oxid Med Cell Longev* 2020: 1215395, 2020.
30. Venugopal K, Ahmadb H, Manikandan E, Thanigai Arul K, Kavithae K, Moodleyf MK, Rajagopal K, Balabhaskar R and Bhaskar M: The impact of anticancer activity upon Beta vulgaris extract mediated biosynthesized silver nanoparticles (ag-NPs) against human breast (MCF-7), lung (A549) and pharynx (Hep-2) cancer cell lines. *J Photochem Photobiol B* 173: 99-107, 2017.
31. Venugopal K, Rather HA, Rajagopal K, Shanthi MP, Sheriff K, Illiyas M, Rather RA, Manikandan E, Uvarajan S, Bhaskar M and Maaza M: Synthesis of silver nanoparticles (Ag NPs) for anticancer activities (MCF 7 breast and A549 lung cell lines) of the crude extract of *Syzygium aromaticum*. *J Photochem Photobiol B* 167: 282-289, 2017.
32. Carlson C, Hussain SM, Schrand AM, Braydich-Stolle LK, Hess KL, Jones RL and Schlager JJ: Unique cellular interaction of silver nanoparticles: Size-dependent generation of reactive oxygen species. *J Phys Chem B* 112: 13608-13619, 2008.
33. Liu X and Feng R: Inhibition of epithelial to mesenchymal transition in metastatic breast carcinoma cells by c-Src suppression. *Acta Biochim Biophys Sin (Shanghai)* 42: 496-501, 2010.
34. Çiftçi H, Türk M, Tamer U, Karahan S and Menemen Y: Silver nanoparticles: cytotoxic, apoptotic, and necrotic effects on MCF7 cells. *Turk J Biol* 37: 9, 2013.
35. Chehelgerdi M, Chehelgerdi M, Allela OQB, Pecho RDC, Jayasankar N, Rao DP, Thamaraiyani T, Vasanthan M, Viktor P, Lakshmaiyi N, et al: Progressing nanotechnology to improve targeted cancer treatment: overcoming hurdles in its clinical implementation. *Mol Cancer* 22: 169, 2023.
36. Karlsson HL, Cronholm P, Gustafsson J and Möller L: Copper oxide nanoparticles are highly toxic: A comparison between metal oxide nanoparticles and carbon nanotubes. *Chem Res Toxicol* 21: 1726-1732, 2008.
37. Dusinska M, Boland S, Saunders M, Juillerat-Jeanneret L, Tran L, Pojana G, Marcomini A, Volkovova K, Tulinska J, Knudsen LE, et al: Towards an alternative testing strategy for nanomaterials used in nanomedicine: Lessons from NanoTEST. *Nanotoxicology* 9 (Suppl 1): S118-S132, 2015.



Copyright © 2024 Konu. This work is licensed under a Creative Commons Attribution-NonCommercial-NoDerivatives 4.0 International (CC BY-NC-ND 4.0) License.